



Pressure Transients in Gas Phase Adsorptive Reactors

BHASKAR K. ARUMUGAM AND PHILLIP C. WANKAT

School of Chemical Engineering, Purdue University, West Lafayette, IN 47907-1283, USA

Abstract. The role of pressure and flow transients caused by strong adsorption on the behavior of gas phase adsorptive reactors was studied using a staged model. The general gas phase reaction $A + B \rightleftharpoons C$ is considered for two cases: (1) the product C is adsorbed and (2) both reactants A and B are adsorbed. Strong adsorption of one or more components causes a decrease in the pressure(s) in the stage(s). The pressure decrease causes variations in the inlet and outlet flow rates and in the case of multiple stages, it causes variations in the flows between tanks. In accordance with Le Chatelier's principle, the pressure decrease aids or inhibits product formation depending on whether there is an increase or decrease in total moles by reaction. Reactant flow into the section where adsorption occurs increases because of increased pressure drop behind the adsorption front. However, the residence time of the reactants behind the adsorption front is lower because of the higher velocity. The flow variations can aid or hinder product formation depending on the specific conditions. Thus, the adsorption-caused pressure variations directly modify reaction rates and product concentrations and, also indirectly, by causing flow variations which affect reaction rates and product concentrations. This study highlights the need to include pressure variations when modeling gas phase adsorptive reactors if adsorption is strong irrespective of the net change in the total moles by reaction. It also demonstrates a method to incorporate axial pressure drop in staged models.

Keywords: adsorptive reactors, pressure transients

Introduction

There is a growing interest in pressure swing (Alpay et al., 1994; Knaebel and Cussler, 1996; Lu and Rodrigues, 1994) and rapid pressure swing (Alpay et al., 1993) adsorptive reactors because they offer many advantages. The attractiveness of adsorptive reactors can be attributed to the following reasons: (1) the thermodynamic limit on equilibrium conversion can be overcome by adsorbing one or more of the products, (2) lower temperatures can be employed, thus reducing catalyst deactivation and energy requirements, and (3) in the case of multiple reactions, selectivity can be enhanced by preferentially adsorbing the desired product. Various theoretical studies of adsorptive reactors have been undertaken (Alpay et al., 1993, 1994; Kirkby and Morgan, 1994; Lu and Rodrigues, 1994). In most studies, axial pressure gradients have been neglected. This is valid under certain circumstances. For example, axial pressure gradients can be neglected for a system

where the feed consists of dilute reactants in an inert nonadsorbing carrier (Alpay et al., 1994).

There are two adsorption situations with no reaction where axial pressure gradients are known to be important. First, significant pressure gradients can occur in cyclic gas adsorption processes with short cycle times (Jones and Keller, 1981; Sundaram and Wankat, 1988). Thus, axial pressure gradients are expected to be significant in rapid pressure swing reactors.

In the second case, large transients in flow and pressure were observed experimentally and theoretically when an adsorbent column presaturated with a relatively weakly adsorbed component (e.g., helium) was loaded with a strongly adsorbed feed mixture (e.g., propane) at the same pressure (Arumugam and Wankat, 1996). In both the experiments and the models the supply tank pressure, not the inlet flow rate, was controlled. Since the entering propane is adsorbed faster than it is fed to the column, the total moles in the gas phase decreases, the column pressure drops, the pressure

difference between the tank and the column inlet increases, and the inlet flow rate increases while the outlet flow rate decreases. Very large pressure decreases and inlet flow rate increases were observed experimentally. Predictions from a single well-stirred tank model agreed qualitatively with single column experiments. A multiple tanks in series model predicted that pressure and flow oscillations occur which last until the feed breaks through. These oscillations become quite small as the number of stages is increased. Experiments conducted with three columns in series showed oscillations in pressure and flow rates.

Adsorption-generated pressure and flow effects are expected to be significant in adsorptive reactors if adsorption of a concentrated component is strong; for example, ammonia synthesis by pressure swing reaction (Knaebel and Cussler, 1996) where the product ammonia is strongly adsorbed. A theoretical study of the effects of these adsorption-caused pressure and flow transients on reaction kinetics and outlet concentrations is presented in this paper.

Model Development

The prototypical gas phase reaction $A + B \rightleftharpoons C$ is considered in two situations: (a) the product C is adsorbed and (b) the reactants A and B are adsorbed. Results for Case A (product adsorbs) are presented for reaction occurring in a single CSTR, three CSTRs in series, and twenty five CSTRs and for Case B (reactants adsorb), results are shown for 25 CSTRs in series only. Twenty five CSTRs in series is expected to be an adequate representation of column behavior (Barker et al., 1983). The model system is shown schematically in Fig. 1. The supply pressure from the feed cylinders and the outlet pressure are set. The inlet flows to each tank and the outlet flow from the last tank are determined by the supply and ambient pressures, tubing dimensions,

and flow characteristics. Due to adsorption, the pressure in each tank and all flows vary. The following assumptions were made: (1) isothermality, (2) local equilibrium, (3) well stirred tanks with constant void fraction, (4) competitive Langmuir isotherms, (5) ideal gas behavior, and (6) gas phase reaction with mass action reaction rate. The results are expected to be qualitatively useful for other stoichiometries and when these assumptions are not valid. Isothermality and this particular stoichiometry will be relaxed in future work.

The material balance for component i ($i = A, B, C, D$, or I) in tank j is given as,

$$\frac{dn_{i,j}}{dt} = y_{i,j-1}F_{\text{connect},j} - y_{i,j}F_{\text{connect},j+1} - \rho_p V_j(1 - \epsilon_e) \frac{dq_{i,j}}{dt} + v_i R_j \quad (1)$$

where, for component i in tank j , $n_{i,j}$ is the total moles in the gas phase, $y_{i,j}$ is the mole fraction, and $q_{i,j}$ is the amount adsorbed; $i = A, B, C, D$ and I and $j = 1 - N$. The stoichiometric coefficient v_i is 1 for the product C, -1 for the reactants A and B and zero for D and I. By changing v_i other reactions of the family $aA + bB \rightleftharpoons cC$ can be studied. The molar flow rate, $F_{\text{connect},j}$, is expressed as

$$F_{\text{connect},j} = \frac{\pi D_{\text{connect},j}^4 (P_{j-1}^2 - P_j^2)}{256 R_g T \mu_{\text{connect},j} L_{\text{connect},j}} \quad (2)$$

where compressible laminar flow has been assumed (Sakiadis, 1984). During the transient period before breakthrough occurs, the flow may not be in the laminar regime and different flow equations will be appropriate. Equation (2) relates the flows and pressure drop between tanks; the connecting tube itself is assumed to have no volume. This is a convenient approach to account for axial pressure drop in staged models. The

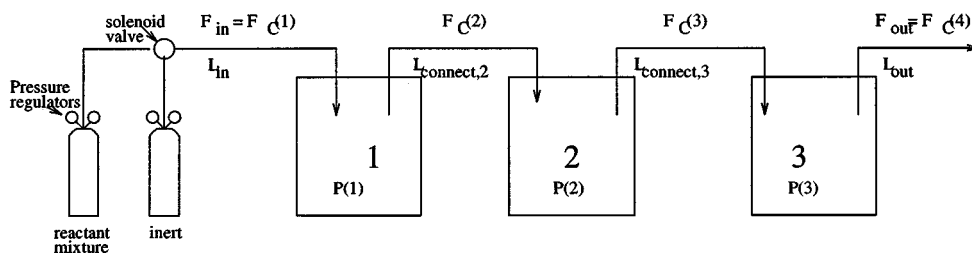


Figure 1. Schematic representation of the staged model.

adsorption of component i is characterized by the competitive Langmuir isotherm:

$$q_{i,j} = \frac{K_i y_{i,j} P_j}{1 + \sum_{k=A,B,C, \text{ or } D} b_k y_{k,j} P_j} \quad (3)$$

Equation (3) is known to be thermodynamically inconsistent unless all K_i/b_i are equal. The rate of reaction R_j is given by

$$R_j = \epsilon_e V_j \rho_p k \left(c_{A,j} c_{B,j} - \frac{c_{C,j}}{K_p} \right) \quad (4)$$

where V_j is the volume of each tank. The ideal gas law for component i is

$$c_{i,j} = \frac{y_{i,j} P_j}{R_g T} = \frac{n_{i,j}}{\epsilon_e V_j}, \quad i = A, B, C, D, \text{ or } I \quad (5)$$

The boundary conditions are: $y_{i,0} = y_{i,\text{in}}$, $P_0 = P_{\text{in}}$, and $P_{N+1} = P_{\text{out}}$.

Speedup, a dynamic plant flowsheeting software, was used to solve the above system of differential algebraic equations (Aspen Technology Inc., 1994). Simulation conditions common to both cases are given in Table 1.

Table 1. Parameters common to all simulations.

Reaction: $A + B \rightleftharpoons C$		
Parameter	Value	Units
Number of tanks	1, 3, or 25	
$L_0 (= L_{\text{in}})$	0.0625	m
$L_N (= L_{\text{out}})$	0.6250	m
$L_{\text{connect},j} (j = 2, N - 1)$	0.15625/number of tanks	m
$D_{\text{connect},j}$	0.0025	m
P_{in}	$4 \times 1.013 \times 10^5$	Pa
P_{out}	1.013×10^5	Pa
R , Gas constant	8.3144	J/mol · K
Temperature	300	K
Viscosity	3.728×10^{-5}	kg/m · s
Tank volume	0.1285/number of tanks	m ³
ϵ_e	0.45	
ρ_p	543	kg/m ³

Table 2. Simulation conditions: Case 1.

Case 1: 60/40/0::A/B/I as feed			
$K_C = 1.7983\text{E} - 4 \text{ mol}/(\text{kg} \cdot \text{Pa})$, $b_C = 3.433\text{E} - 4 \text{ Pa}^{-1}$			
Run	Figure numbers	Rate const., k , m ⁶ /(kg catalyst · mol · s)	Equil. const., K_p (mol/m ³) ⁻¹
Case 1.1.1	2	3.7084E-7	9.931E-3
Case 1.3.1	3	1.8542E-7	9.931E-1
Case 1.25.1	4, 5, 6, 7	1.8542E-7	9.931E-1

Results

Case 1: Product C Adsorbs

In this case, a 60/40 feed mixture of nonadsorbed A and B reacts to form a strongly adsorbed product C. Other simulation conditions are listed in Table 2.

An adsorptive reactor would be used in this situation to enhance equilibrium conversion, to achieve higher conversion at lower temperature, or both. High adsorptive capacity for C is required to make the process feasible. Following saturation of the bed with C, a rinse step with C at a lower temperature to arrest reverse reaction, can be incorporated. Product C can then be recovered (and the bed regenerated) during subsequent blowdown and vacuum or purge steps. Such a scheme has been proposed for NH₃ production (Knaebel and Cussler, 1996).

Single CSTR. The tank initially containing inert I at 1 atm is pressurized with I from a source at 4 atm. At $t = 1000\text{s}$, the inlet flow is switched to the feed gas from a source at 4 atm.

The concentration of A (Fig. 2) initially increases rapidly because of the high inlet flow which contains A in excess; it decreases after the adsorbent is saturated and the inlet flow rate reduces to a steady value. Equations (4) and (5) show that pressure decrease causes a decrease in concentrations and hence in the forward reaction rate. However, this is more than compensated for by the increase in inlet flow rate (Eq. (2)) caused by the pressure decrease, and the inhibition of the reverse reaction by adsorption of C. The concentration of B (Fig. 2) increases initially because the inlet flow rate is high, and then decreases since it is the limiting reactant. After the adsorbent is saturated, the reverse reaction increases and the concentration of B increases again until it reaches a steady value. Neglecting the

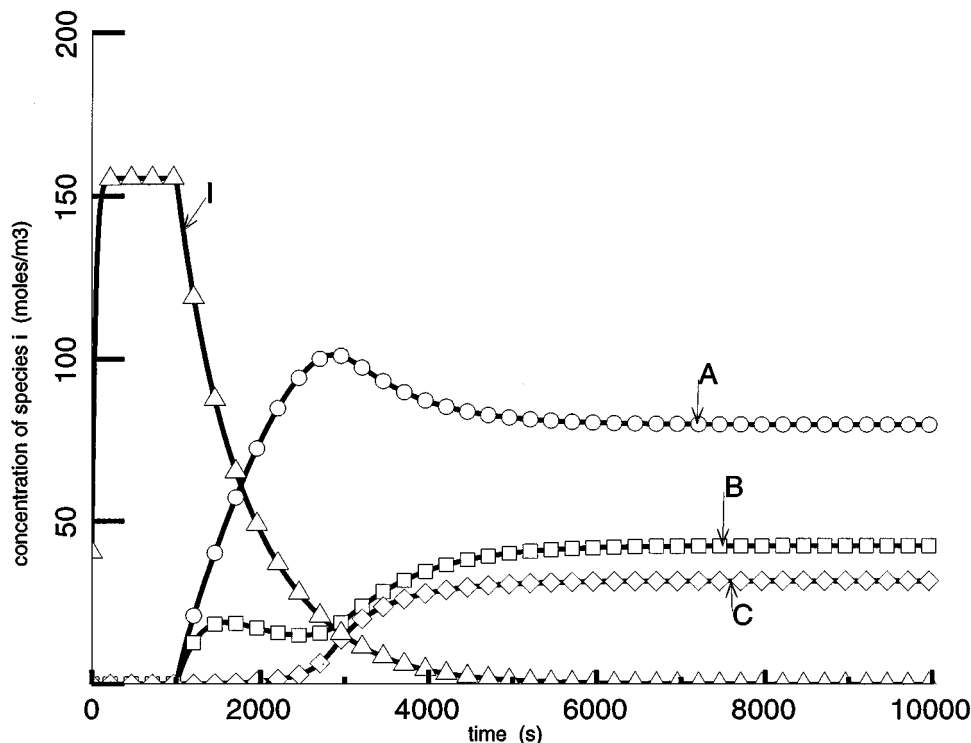


Figure 2. Concentration variations in a single CSTR with the product C adsorbing. The tank is pressurized with inert from a source at 4 atm. Flow is switched at $t = 1000$ s to a 60/40 feed of A/B. See Tables 1 and 2.

effect of pressure transients will result in an incorrect prediction of the amount of product formed during the transient period.

Three CSTRs. The three tanks initially contain inert, I, at 1 atm. The system is pressurized with the inert from a source at 4 atm and then the flow is switched to a 60/40 feed mixture of A/B from a source at 4 atm.

Typical results are shown in Fig. 3. The peak in the outlet concentration of A is again a result of high flow rate containing an excess of A entering tank 3 from tank 2 when adsorption occurs in tank 3. The outlet concentration of B exhibits two smaller peaks which corresponds to the oscillations observed when only adsorption occurs.

Twenty Five CSTRs. The results with 25 CSTRs in series are a good approximation to the performance of a single column. The outlet concentrations are shown in Fig. 4. A concentration peak of component A exists ahead of the adsorption front of C. This relatively pure A could be recycled. The concentration profiles of components A, B, and C are shown in Figs. 5, 6, and 7.

Because of the pressure variation, the flow rate is high behind the adsorption front of C and low ahead of this front. Behind the adsorption front the gas is mostly A and B since C is adsorbed. Since C is adsorbed and B is the limiting reactant, a region containing mostly A moves ahead of the adsorption front. After the adsorbent is saturated, C starts accumulating in the gas phase and the reverse reaction increases. Hence, the concentration of B increases. As a result, a small peak in the concentration of B moves down the column simultaneously with the C peak (compare Figs. 6 and 7). As the reverse reaction is higher behind the adsorption front, a peak in the rate of formation of C moves with the adsorption front. Additional results for 1, 3, and 25 CSTRs are presented by Arumugam (1996). Ignoring the pressure and flow effects will give incorrect predictions in all these cases.

Case 2: Both A and B Adsorb

In this case both reactants A and B adsorb; the product C and the presaturant I are nonadsorbing. The feed is a 60/40 mixture of A/B. A, which is

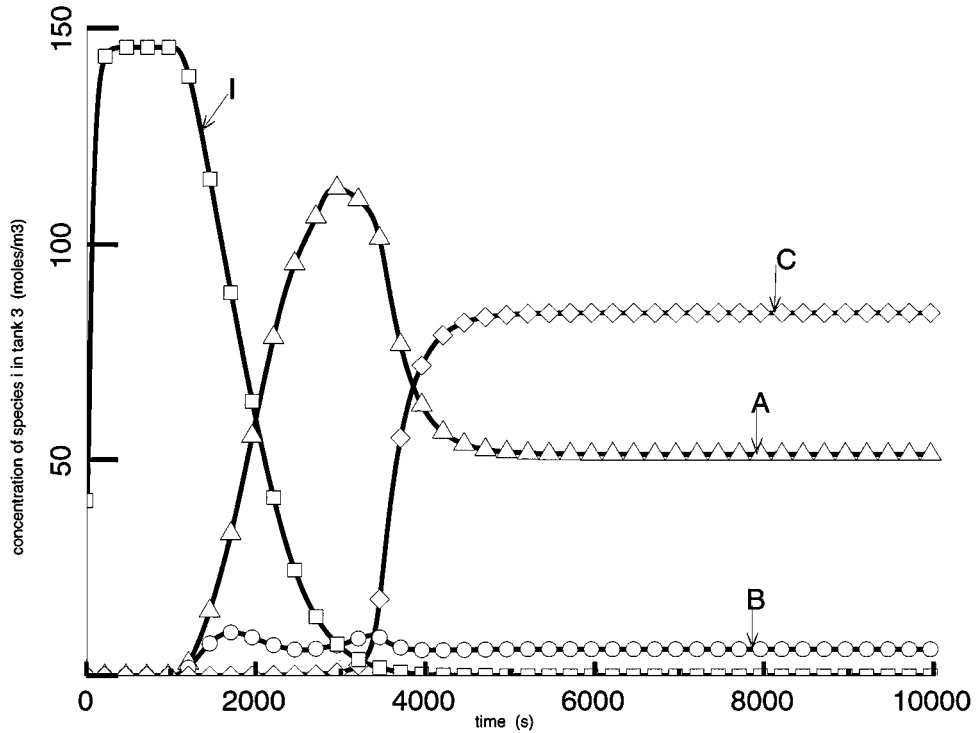


Figure 3. Outlet concentrations for the case of three CSTRs in series with the product C adsorbing. The first tank is pressurized with inert from a source at 4 atm. Flow is switched at $t = 1000$ s to a 60/40 feed of A/B. See Tables 1 and 2.

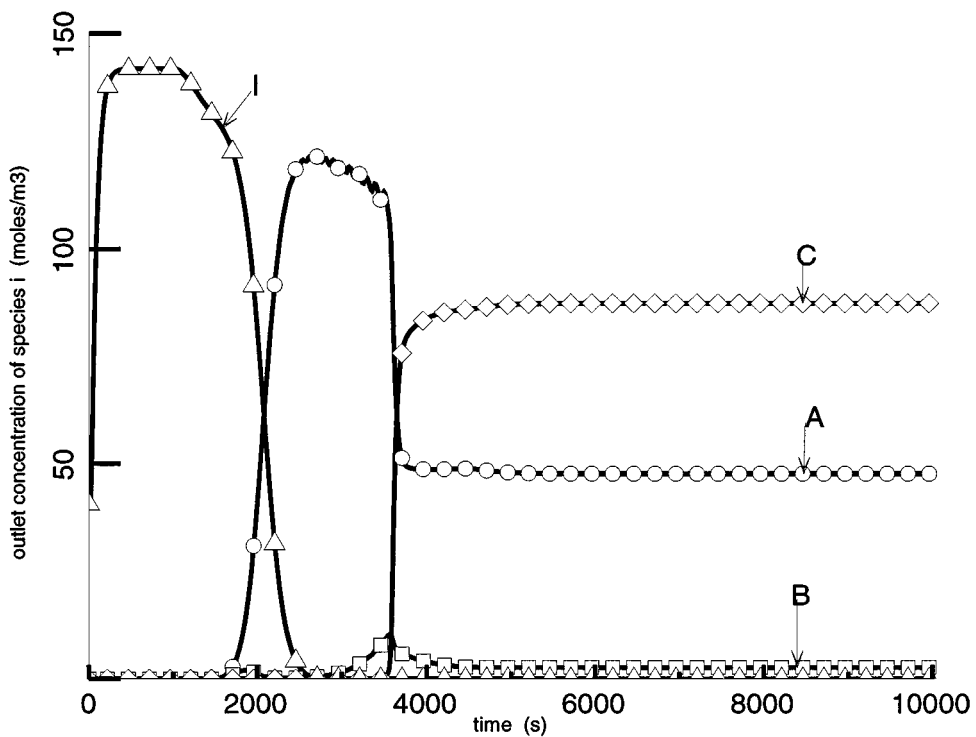


Figure 4. Outlet concentrations for twenty five CSTRs in series with the product C adsorbing. The first tank is pressurized with inert from a source at 4 atm. Flow is switched at $t = 1000$ s to a 60/40 feed of A/B. See Tables 1 and 2.

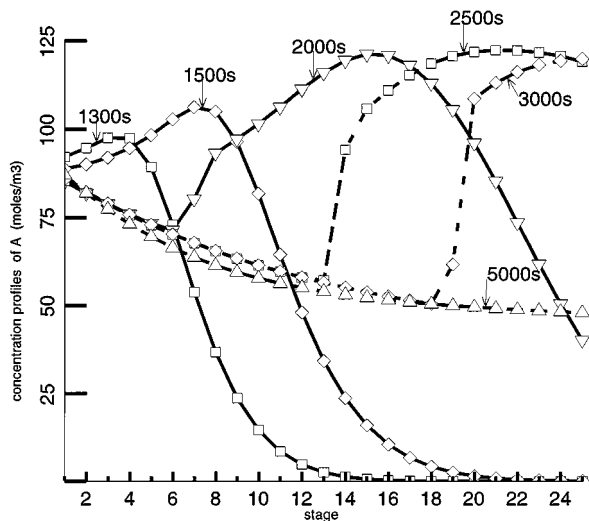


Figure 5. Concentration profiles of reactant A for twenty five CSTRs in series with the product C adsorbing. The first tank is pressurized with inert from a source at 4 atm. Flow is switched at $t = 1000$ s to a 60/40 feed of A/B. See Tables 1 and 2.

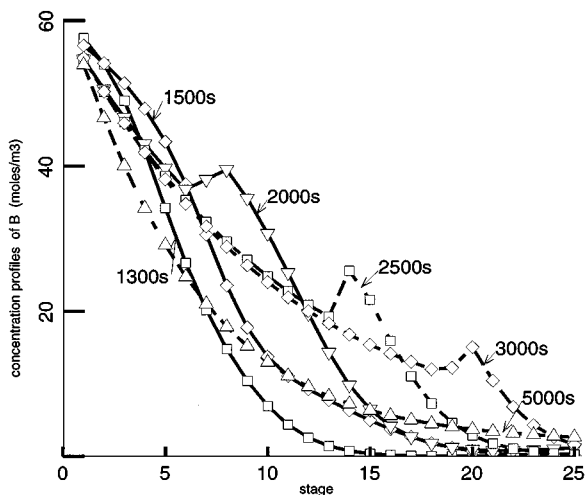


Figure 6. Concentration profiles of reactant B for twenty five CSTRs in series with the product C adsorbing. The first tank is pressurized with inert from a source at 4 atm. Flow is switched at $t = 1000$ s to a 60/40 feed of A/B. See Tables 1 and 2.

present in excess, adsorbs less strongly than B. Further details of the simulation conditions are given in Table 3.

Twenty Five CSTRs. Pressure profiles are shown in Fig. 8. At each axial position, the total pressure decreases rapidly until the shock front reaches that location and decreases relatively slowly after the shock

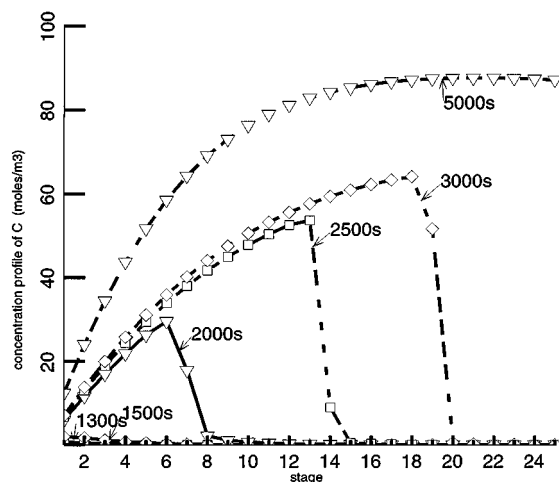


Figure 7. Concentration profiles of the adsorbing product C for twenty five CSTRs in series. The first tank is pressurized with inert from a source at 4 atm. Flow is switched at $t = 1000$ s to a 60/40 feed of A/B. See Tables 1 and 2.

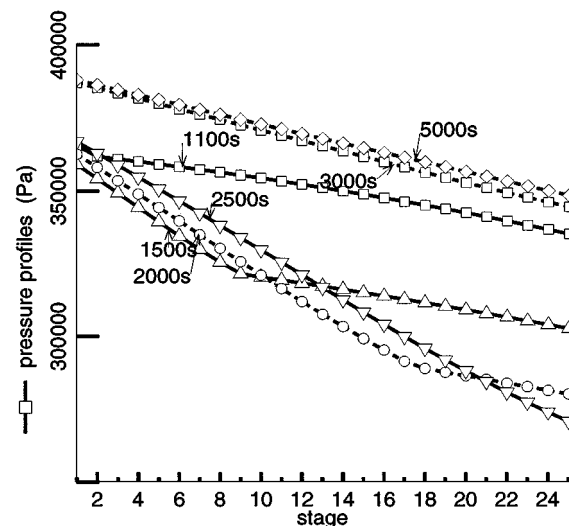


Figure 8. Pressure profiles for twenty five CSTRs in series with both A and B adsorbing. The first tank is pressurized from an initial pressure of 1 atm with inert from a source at 4 atm. Flow is switched at $t = 1000$ s to a 60/40 feed of A/B. See Tables 1 and 3.

front passes. These results are expected for CSTRs in series with only adsorption (Arumugam and Wankat, 1996). There is a discontinuity in the slope of the pressure profile at the location of the shock front. Behind the adsorption front the gradient is steeper than it would be without reaction because there is a decrease in total moles due to reaction. After breakthrough occurs the pressure profile becomes steady though with a steeper

Table 3. Simulation conditions: Case 2.

CASE 2: 60/40::A/B as feed			
$K_A = 1.7983E - 4 \text{ mol}/(\text{kg} \cdot \text{Pa})$, $b_A = 3.433E - 4 \text{ Pa}^{-1}$ $K_B = 2.8385E - 4 \text{ mol}/(\text{kg} \cdot \text{Pa})$, $b_B = 5.216E - 5 \text{ Pa}^{-1}$			
Run	Figure numbers	Rate const., k , $\text{m}^6/(\text{kg catalyst} \cdot \text{mol} \cdot \text{s})$	Equil. const., K_p $(\text{mol}/\text{m}^3)^{-1}$
Case 2.25.1	8, 9, 10, 11, 12,	$1.8542E-8$	$9.931E-1$
Case 2.25.2	13	$1.8542E-7$	$9.931E-1$

gradient compared to when reaction is absent. The flow (Fig. 9) behind the shock front is much higher than ahead of the shock front. The decrease in total moles at the reaction front causes a minimum in molar flow rate. Once the shock front leaves the column, the pressure recovers (Fig. 8) and the flowrate drops to a steady value (Fig. 9).

The concentration profiles of A, B, and C are shown in Figs. 10, 11, and 12. The adsorbent becomes saturated with A earlier than with B, and A accumulates in the gas phase. Desorption of A due to the competitive adsorption of B causes a peak in the concentration of A (Fig. 10). Nonadsorbed C moves ahead of the adsorption front and hence there is a peak in the concentration of C (Fig. 12). If the reverse reaction rate is low, there may be a period with pure C is obtained as product (Fig. 13, $k = 1.8542 \times 10^{-7} \text{ m}^6/(\text{kg catalyst} \cdot \text{mol} \cdot \text{s})$)

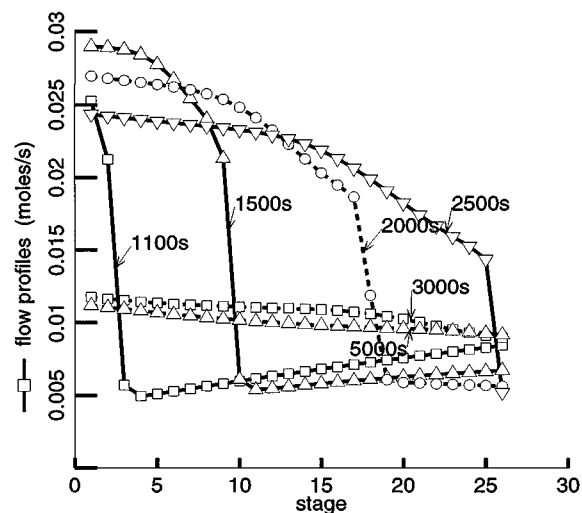


Figure 9. Flow profiles for twenty five CSTRs in series with both A and B adsorbing. The first tank is pressurized from an initial pressure of 1 atm with inert from a source at 4 atm. Flow is switched at $t = 1000\text{s}$ to a 60/40 feed of A/B. See Tables 1 and 3.

which is ten times the rate in other figures). The rate of formation of C behind the adsorption front is lower during the transient period before breakthrough occurs because of lower tank pressure; it increases once breakthrough of A occurs and the pressure increases. If there is a net increase in total moles by reaction, the rate of product formation will be higher during the transient period before breakthrough occurs. Additional results are given by Arumugam (1996).

Discussion

If there is reaction and no adsorption, the nature of pressure transients changes. In a single CSTR, the pressure and flow minima disappear when adsorption is absent. Oscillations in pressure and flow and the resulting waviness in product concentrations for the three CSTR system were not observed when there is no adsorption. Similarly, the peaks in concentrations and reaction rates (not shown) moving down the column in the twenty five CSTRs in series model disappear if there is no adsorption. It appears that oscillations occur only when the sink has a finite capacity for the component removed.

Results with adsorption present with no reaction agreed with the results of Arumugam and Wankat (1996). Steady state mass balances were made for Case B (A and B adsorb) with single, three, and twenty five stages for a 60/40 feed of A/B. The error was less than 1% for all three cases.

Reaction stoichiometries with no volume change ($A + B \rightleftharpoons 2C$) and with an increase in volume ($A + B \rightleftharpoons 4C$) with A and B adsorbing were also investigated (Arumugam, 1996). Since the focus was on the effect of volume changes only, Eq. (4), without any changes, was used to describe reaction kinetics. The results for single and three stages are qualitatively similar to Cases 1 and 2. However, the flow increase during the transient period is lower because there is no decrease

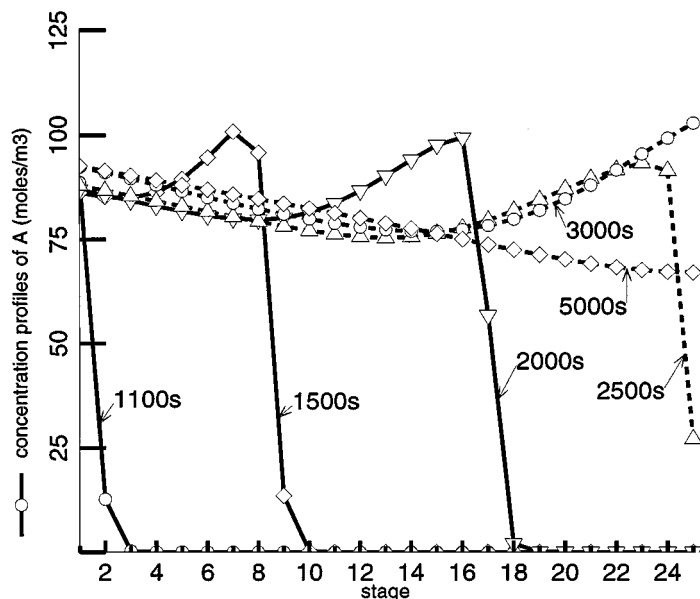


Figure 10. Concentration profiles of A for twenty five CSTRs in series with both A and B adsorbing. The first tank is pressurized from an initial pressure of 1 atm with inert from a source at 4 atm. Flow is switched at $t = 1000$ s to a 60/40 feed of A/B. See Tables 1 and 3.

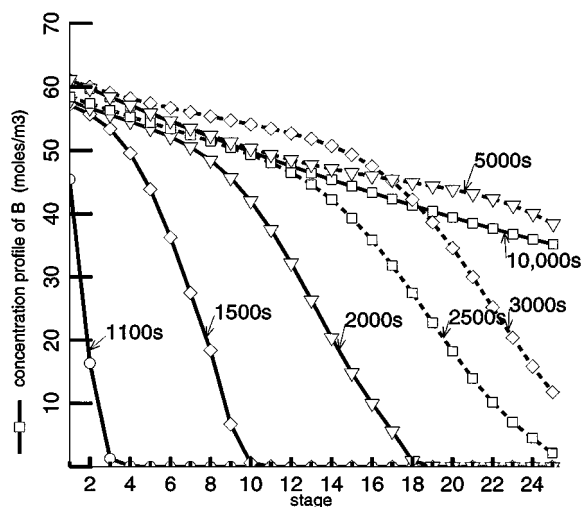


Figure 11. Concentration profiles of B for twenty five CSTRs in series with both A and B adsorbing. The first tank is pressurized from an initial pressure of 1 atm with inert from a source at 4 atm. Flow is switched at $t = 1000$ s to a 60/40 feed of A/B. See Tables 1 and 3.

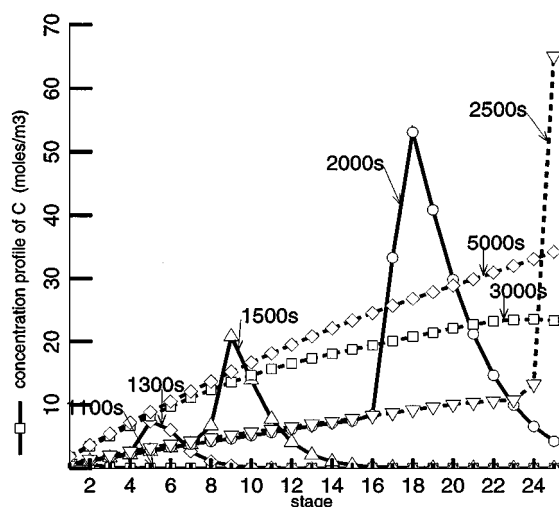


Figure 12. Concentration profiles of product C for twenty five CSTRs in series with both A and B adsorbing. The first tank is pressurized from an initial pressure of 1 atm with inert from a source at 4 atm. Flow is switched at $t = 1000$ s to a 60/40 feed of A/B. See Tables 1 and 3.

in volume by reaction. The effect of lower flow is notable with twenty five stages—breakthrough takes much longer and higher conversions are obtained during transience because the residence time is greater. The discontinuity in slopes of pressure profiles (Fig. 8) was not observed.

Simulations were also done for system where A, B, and C do not adsorb, but a nonreacting species in the feed D does adsorb (Arumugam, 1996). The results obtained are what one would expect by superimposing a pure reaction system ($A + B \rightleftharpoons C$) and a pure adsorption system (D replaces I).

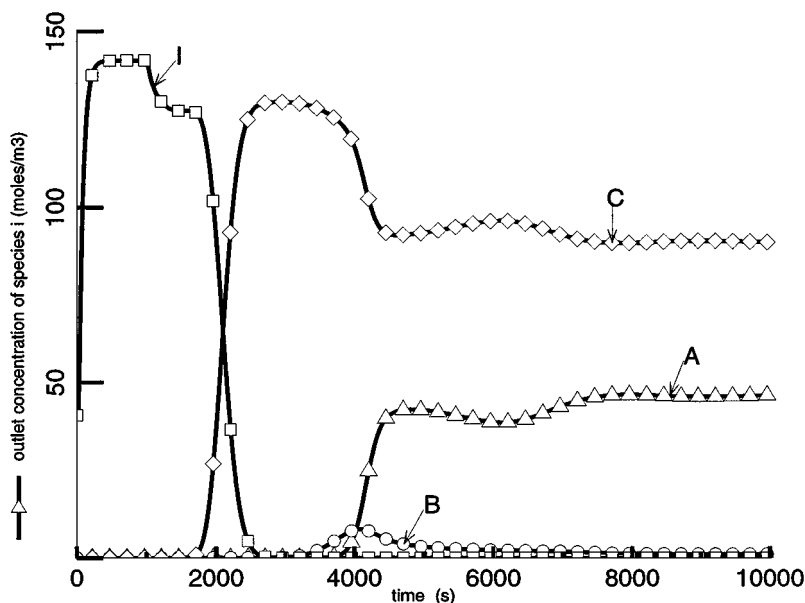


Figure 13. Outlet concentrations for twenty five CSTRs in series with both A and B adsorbing. Rate constant, k , $= 1.8542 \times 10^{-7} \text{ m}^6/(\text{kg} \cdot \text{s})$. The first tank is pressurized from an initial pressure of 1 atm with inert from a source at 4 atm. Flow is switched at $t = 1000\text{s}$ to a 60/40 feed of A/B. See Tables 1 and 3.

The most restrictive assumption in the model is isothermality. The heat of adsorption and reaction will influence the performance of an adsorptive reactor. For instance, endothermic reactions will tend to lower temperature, thus enhancing adsorption capacity. The heat of adsorption, in turn, aids the reaction. However, the heat generated from an exothermic reaction will lower the adsorption capacity and the heat of adsorption will hinder product formation if equilibrium controls.

Mass transfer resistances will reduce the magnitude of pressure and flow transients. This model is applicable to heterogeneous reactions if the pseudo-homogeneous assumption is valid.

Conclusions

The occurrence of adsorption-caused pressure gradients and flow rate changes will modify reaction rates and product concentrations in a concentrated gas phase adsorptive reactor. The pressure transients may aid or hinder product formation depending on the volume change by reaction in accordance with Le Chatelier's principle. Axial pressure gradients need to be included in adsorptive reactor modeling when there is a high concentration of strongly adsorbed species. Further research is needed to study the effects of heat of reaction and finite heat and mass transfer rates.

Nomenclature

A, B	Reactants	—
b	Constant in Langmuir isotherm	Pa^{-1}
C	Product	—
c	Gas phase concentration	mol/m^3
D	(1) Tube diameter (2) Non-reacting but adsorbing component in feed	m
F	Flow rate	mol/s
I	Inert	—
k	Reaction rate constant	$\text{m}^6/\text{kg catalyst} \cdot \text{mol} \cdot \text{s}$
K	Constant in Langmuir isotherm	$\text{mol}/\text{kg} \cdot \text{Pa}$
K_p	Equilibrium constant	$(\text{mol}/\text{m}^3)^{-1}$
L	Tube length	m
n	Moles in gas phase	mol
P	Pressure	Pa
q	Amount adsorbed	mol/kg
R_g	Gas constant,	$\text{Joules}/\text{mole} \cdot \text{K}$
R	Rate of formation of product	mol/s
t	Time	s
T	Temperature	$\text{K} [1.5\text{pt}]$

V	Total volume of each tank	m^3
y	Mole fraction in gas phase	—

Greek Letters

ϵ_e	Interstitial void fraction	—
μ	Gas viscosity	$\text{kg/m} \cdot \text{s}$
ρ_p	Particle density	kg/m^3
ν	Stoichiometric coefficient	—

Subscripts

A, B	Reactants	—
C	Product	—
connect, j	Refers to connecting tube	—
D	Non-reacting, adsorbing component in feed	—
i	Component i	—
in	Inlet conditions	—
j	Tank j	—
I	Nonreacting, nonadsorbing inert component	—
out	Outlet conditions	—

Acknowledgment

This research was partially supported by NSF Grant CTS-9401935. Discussions with Drs. Kent Knaebel and Jim Ritter were very helpful.

References

- Alpay, E., D. Chatsiriwech, L.S. Kershenbaum, C.P. Hull, and N.F. Kirkby, "Combined Reaction and Separation in Pressure Swing Processes," *Chemical Engineering Science*, **49**(24B), 5845–5864 (1994).
- Alpay, E., C.N. Kenney, and D.M. Scott, "Simulation of Rapid Pressure Swing Adsorption and Reaction Processes," *Chemical Engineering Science*, **48**(18), 3173–3186 (1993).
- Arumugam, B.K., "Bulk Multicomponent Adsorption and Pressure Transients in Adsorption Systems," PhD thesis, Purdue University, West Lafayette, IN (1996).
- Arumugam, B.K. and P.C. Wankat, "Pressure Behavior During the Loading of Adsorption Systems," *Fundamentals of Adsorption*, M.D. LeVan (Ed.), pp. 51–58, Kluwer Academic Publishers, Massachusetts, 1996.
- Barker, P.E., K. England, and G. Vlachogiannis, "Mathematical Model for the Fractionation of Dextran on a Semi-Continuous Counter-Current Simulated Moving Bed Chromatograph," *Chem. Eng. Res. Des.*, **61**, 241–247 (1983).
- Jones, R.L. and G.E. Keller, "Pressure-Swing Parametric Pumping—A New Adsorption Process," *J. Separ. Proc. Technol.*, **2**(3), 17–23 (1981).
- Kirkby, N.F. and J.E.P. Morgan, "A Theoretical Investigation of Pressure Swing Reaction," *Trans IChemE*, **72**, Part A, 541–550 (1994).
- Knaebel, K.S. and E.L. Cussler, "A Novel Pressure Swing Adsorption System for Ammonia Synthesis," *Fundamentals of Adsorption*, M.D. LeVan (Ed.), pp. 457–464, Kluwer Academic Publishers, Massachusetts, 1996.
- Lu, Z.P. and A.E. Rodrigues, "Pressure Swing Adsorption Reactors: Simulation of Three-Step One-Bed Process," *AIChE Journal*, **40**(7), 1118–1137 (1994).
- Sakiadis, B.C., *Fluid and Particle Mechanics*, Perry's Chemical Engineers' Handbook, Section 5, 6th edition. McGraw-Hill, N.Y., 1984.
- Sundaram, N. and P.C. Wankat, "Pressure Drop Effects in the Pressurization and Blowdown Steps of Pressure Swing Adsorption," *Chemical Engineering Science*, **43**(1), 123–129 (1988).